

**Precipitation  
seasonality effects  
on ice core isotope  
records**

W. J. van de Berg et al.

# The effect of precipitation seasonality on Eemian ice core isotope records from Greenland

W. J. van de Berg<sup>1</sup>, M. R. van den Broeke<sup>1</sup>, E. van Meijgaard<sup>2</sup>, and F. Kaspar<sup>3</sup>

<sup>1</sup>IMAU, Utrecht University, Utrecht, The Netherlands

<sup>2</sup>KNMI, De Bilt, The Netherlands

<sup>3</sup>Deutscher Wetterdienst (DWD), Offenbach, Germany

Received: 17 December 2012 – Accepted: 4 January 2013 – Published: 17 January 2013

Correspondence to: W. J. van de Berg (w.j.vandenberg@uu.nl)

Published by Copernicus Publications on behalf of the European Geosciences Union.

Title Page

Abstract

Introduction

Conclusions

References

Tables

Figures

⏪

⏩

◀

▶

Back

Close

Full Screen / Esc

Printer-friendly Version

Interactive Discussion

## Abstract

The previous interglacial (Eemian, 130–114 kyr BP) had a mean sea level highstand 4 to 7 m above the current level, and, according to climate proxies, a 2 to 6 K warmer Arctic summer climate. Greenland ice cores extending back into the Eemian show a reduced depletion in  $\delta^{18}\text{O}$  of about 3‰ for this period, which suggests a significant warming of several degrees over the Greenland ice sheet. Since the depletion in  $\delta^{18}\text{O}$  depends, among other factors, on the condensation temperature of the precipitation, we analyze climatological processes other than mean temperature changes that influence condensation temperature, using output of the regional climate model RACMO2. This model is driven by ERA-40 reanalysis and ECHO-G GCM boundaries for present-day, preindustrial and Eemian climate. The processes that affect the condensation temperature of the precipitation are analyzed using 6-hourly model output. Our results show that changes in precipitation seasonality can cause significant changes of up to 2 K in the condensation temperature that are unrelated to changes in mean temperature.

## 1 Introduction

Isotope records from ice cores provide a high resolution record of past climate. Because stable heavy water isotopes, i.e.  $^{18}\text{O}$  and D, favor the liquid and solid phase above the gas phase slightly more than their lighter and more abundant species,  $^{16}\text{O}$  and H, evaporation causes a depletion of the heavy isotopes, and subsequent condensation reinforces this in the water vapor. For an air parcel traveling poleward and cooling, the relative depletion of stable heavy isotopes is then an indirect measure of temperature (Dansgaard, 1964).

Several ice cores drilled in Greenland, for example, GRIP and NorthGRIP, provide a record of past climate with annual resolution, extending back into the Eemian, 130 to 114 kyr BP (Johnsen et al., 1992; NorthGRIP community members, 2004). Ice

## Precipitation seasonality effects on ice core isotope records

W. J. van de Berg et al.

Title Page

Abstract

Introduction

Conclusions

References

Tables

Figures



Back

Close

Full Screen / Esc

Printer-friendly Version

Interactive Discussion



cores drilled in Antarctica extend even further back in time, but have a lower temporal resolution due to the smaller accumulation rates (Petit et al., 1999; EPICA community members, 2004). In these ice cores, the depletion of stable isotopes like  $^{18}\text{O}$  and D provide an unique measure of past temperatures. However, isotopes are no direct measure of near surface air temperature or mean atmospheric temperature. The precipitation that ends up in an ice core has taken different paths and originates from different latitudes, so no simple relation is expected between temperature and isotopic depletion (e.g. Jouzel et al., 1997; Helsen et al., 2004). After snow deposition, surface snow processes alter the isotopic signal, and diffusion damps within the snowpack the seasonal signal (Helsen et al., 2006; Steen-Larsen et al., 2011).

Various Greenland ice cores show lower rates of depletion for the Eemian, suggesting that the Greenland Ice Sheet had a significantly warmer climate during the Eemian than today (Johnsen et al., 1997). For example, Eemian  $\delta^{18}\text{O}$  values at NorthGRIP are about 3‰ higher than present (NorthGRIP community members, 2004), which suggest an Eemian warming of 5 K. In contrast, proxies outside Greenland indicate a 2 to 4 K summer warming during the Eemian (Kaspar and Cubasch, 2007; Otto-Bliesner et al., 2006). General Circulation Model (GCM) and Regional Climate Model (RCM) simulations that compare well with Eemian proxy data outside Greenland show only a moderate 1 K annual warming over Greenland (Kaspar et al., 2005; van de Berg et al., 2011). This discrepancy could be due to model shortcomings, but also due to processes that influenced the dependency of isotope depletion on atmospheric temperature, the so-called isotope thermometer. Jouzel et al. (1997) studied the temporal variability of the isotopic thermometer, highlighting the effect of changes in moisture source elevation, precipitation seasonality and inversion layer strength. For example, summer precipitation in Greenland generally exceeds winter precipitation (Shuman et al., 2001; Sjolte et al., 2011), introducing a warm bias in the isotope thermometer. During the last glacial maximum, changes in this ratio also significantly affected the isotopic signal (Werner et al., 2000). For the Eemian, Masson-Delmotte et al. (2011) showed that precipitation seasonality can have a 1‰ effect on  $\delta^{18}\text{O}$ .

## Precipitation seasonality effects on ice core isotope records

W. J. van de Berg et al.

[Title Page](#)[Abstract](#)[Introduction](#)[Conclusions](#)[References](#)[Tables](#)[Figures](#)[⏪](#)[⏩](#)[◀](#)[▶](#)[Back](#)[Close](#)[Full Screen / Esc](#)[Printer-friendly Version](#)[Interactive Discussion](#)

## Precipitation seasonality effects on ice core isotope records

W. J. van de Berg et al.

Title Page

Abstract

Introduction

Conclusions

References

Tables

Figures

⏪

⏩

◀

▶

Back

Close

Full Screen / Esc

Printer-friendly Version

Interactive Discussion



In this study, the impacts of atmospheric circulation and local precipitation processes on current and Eemian isotopic signals in Greenland are analyzed. For this, the condensation temperature ( $T_c$ ) of the precipitation is calculated. Since the isotopic depletion of precipitation is not simulated in the model, the impact of changing moisture trajectories and moisture origin on the isotopic signal is not included. Rather,  $T_c$  includes the effect of precipitation seasonality, climatic and atmospheric conditions during precipitation events and the effect of condensation altitude on the isotopic signal.

Section 2 gives a description of the model that has been used for this study and the method to derive  $T_c$ . Section 3 discusses the processes that cause the differences between  $T_c$  and  $T_{2m}$  in the present climate. In Sect. 4, we analyze how these processes changed during the Eemian. From these results, conclusions are drawn about the uncertainties that arise if Greenland ice core records are used to estimate local Eemian temperatures.

## 2 Data and methods

### 2.1 Model and simulation set-up

We use present-day, preindustrial and Eemian simulations with the regional atmospheric climate model RACMO2, version 2.1 of the Royal Netherlands Meteorological Institute (KNMI). RACMO2 is a combination of two numerical weather prediction models: the atmospheric dynamics originate from the High Resolution Limited Area Model (HiRLAM, version 5.0.6; Undén et al., 2002), while the description of the physical processes is adopted from the global model of the European Centre for Medium-Range Weather Forecasts (ECMWF, updated cycle 23r4; White, 2001). The general adjustments to the original formulas of the dynamical and physical schemes in RACMO2 are described in detail by van Meijgaard et al. (2008). In addition, for the model version RACMO2, several adjustments have been made to better represent the conditions in the Arctic region, as described in Reijmer et al. (2004) and Ettema et al. (2010b). The

## Precipitation seasonality effects on ice core isotope records

W. J. van de Berg et al.

Title Page

Abstract

Introduction

Conclusions

References

Tables

Figures

⏪

⏩

◀

▶

Back

Close

Full Screen / Esc

Printer-friendly Version

Interactive Discussion



model uses a dynamic multilayer snow model that includes all relevant sub-surface processes on an ice sheet, i.e. snow/ice melt, meltwater percolation, sub-surface meltwater refreezing, meltwater runoff and snow densification due to compaction and re-freezing. Ettema et al. (2009, 2010a,b) showed that RACMO2 accurately simulates the present-day climate of the GrIS. The bias in the annual mean 2 m temperature is only +0.9 K ( $r = 0.99$ ) and the present-day snow accumulation correlates very well with observations from snow pits and firn cores ( $r = 0.95$ ).

For the present-day simulation, RACMO2 was forced with ECMWF Re-Analysis (ERA-40) boundaries: for the preindustrial and Eemian simulations, weather boundaries from the general circulation model ECHO-G were used. ERA-40 covers the period from september 1957 to mid 2003 (Uppala et al., 2005) at a horizontal resolution of about  $1.125^\circ$ . Data from the period 1960–1989 are used here, since this period ends before the observed recent warming of Greenland which started around 1990 (van den Broeke et al., 2009). The ECHO-G model (Legutke and Voss, 1999; Legutke and Maier-Reimer, 1999) consists of the ECHAM4 atmosphere model coupled to the HOPE-G ocean model. The atmosphere model has a horizontal resolution of approximately  $3.75^\circ$  (T30), and 19 levels in the vertical. The individual simulations comprise several thousand years; Kaspar et al. (2005, 2007) and Kaspar and Cubasch (2007) describe these ECHO-G simulations in detail. The climate simulated by ECHO-G has significant decadal variability, and periods with a representative 30 yr-mean climate within the whole ECHO-G run were chosen to force the RCM simulations.

The coupling of RACMO2 to ERA-40 and ECHO-G is achieved by one-way nesting (van de Berg et al., 2011). At the lateral boundaries, prognostic atmospheric fields force the model every 6 h, while the interior of the domain is allowed to evolve freely. The simulation of the present-day climate was run on a stereographic grid with a resolution of  $0.1^\circ$  (11 km); the preindustrial and Eemian simulation were run with a resolution of  $0.165^\circ$  (18 km). Sea-ice fractions and sea surface temperature were interpolated from the corresponding ERA-40 and ECHO-G grids. The snow/ice pack temperature was initialized using the parameterization of Reeh (1991), including the correction for

## Precipitation seasonality effects on ice core isotope records

W. J. van de Berg et al.

Title Page

Abstract

Introduction

Conclusions

References

Tables

Figures

⏪

⏩

◀

▶

Back

Close

Full Screen / Esc

Printer-friendly Version

Interactive Discussion

refreezing. The present-day model integration covers the whole ERA-40 period. Spin-up time is provided by rerunning the first year of ERA-40 three times. For the ECHO-G driven simulations, the first year is omitted to remove the atmospheric spin-up that occurs in the first days after initialization. In these two simulations, the greenhouse gas concentrations were adapted to the historical rates. For the Eemian simulation, orbital settings at 125 kyr BP were applied (Table 1). The ECHO-G driven preindustrial simulation is a few degrees colder over Greenland than the ERA-40 driven recent-past simulation (Fig. S1a), both near the surface as through the troposphere. The impact of these differences on the results will be discussed later in this manuscript.

Limited data are available for the evaluation of the reconstructed Eemian climate. As shown in Kaspar et al. (2005), the ECHO-G output compares very well with pollen data available for Europe, which indicates a 1 to 2 K July warming and a –1 to 3 K January warming. Kaspar et al. (2005) concluded for Europe that statements which characterize the Eemian as overall warmer than today are too simplistic. Francis et al. (2006) analysed lake temperatures on Baffin Island, Arctic Canada, and found 5 to 10 K higher summer lake water temperatures during the Eemian than observed now. RACMO2 simulates about 3 to 4 K July warming for Eastern Baffin Island compared to the preindustrial climate (not shown). However, as noted in Francis et al. (2006), summer lake temperatures exceed air temperatures due to the direct heating of the lake water by sunlight. This lake-atmosphere difference must have been larger in the Eemian because of the stronger summer insolation, which might explain the difference between the proxy data and model output.

## 2.2 Derivation of the condensation temperature

Since RACMO2 does not explicitly calculate water vapor fractionation, the condensation temperature  $T_c$  is used as a measure for  $\delta^{18}\text{O}$ .  $T_c$  is the weighted mean temperature of the model levels of which the precipitation is formed. In a model time step of 10 to 15 min, most of the cloud liquid and ice water content (CWC) that is formed rains out directly. Advection of CWC is a minor contribution to the local precipitation flux

(< 10%). It is thus assumed that the vertical gradient of the precipitation flux is a good measure of the local total condensation. Moreover, CWC is advected along the same trajectory as temperature. Therefore, temperature differences along the cloud content trajectory will be small.

In order to calculate the condensation temperature, daily profiles of precipitation fluxes, 6 hourly temperature profiles and 6 hourly surface precipitation fluxes were used. For each 6 h, the condensation temperature of the precipitation was determined, using the mean temperature for this 6 h and the daily profile of the precipitation flux. A similar approach that used daily precipitation values and mean daily temperatures gave very similar results. This test demonstrates that variability on time scales shorter than a day do not significantly influence the condensation temperature of precipitation.

The condensation temperature  $T_c$  at time  $t$  is defined as

$$(T_c)_t = \frac{\int_0^\infty T_{tz} C_{tz} dz}{\int_0^\infty C_{tz} dz} = \frac{1}{P_t} \int_0^\infty T_{tz} C_{tz} dz, \quad (1)$$

in which  $C_{tz}$  and  $T_{tz}$  are the net precipitation formation and the temperature at level  $z$  and time  $t$ , respectively. The integrated precipitation formation,  $\int_0^\infty C_{tz} dz$ , equals the net precipitation  $P_t$ . Precipitation that evaporates during descent is not counted, therefore  $C_{tz}$  represents the condensate that reaches the surface. By integrating  $(T_c)_t$  over several decades, thus

$$T_c = \frac{\int_0^T \int_0^\infty T_{tz} C_{tz} dz dt}{\int_0^T P_t dt} = \frac{1}{P} \int_0^T \int_0^\infty T_{tz} C_{tz} dz dt,$$

the effects of seasonal and inter annual variability are included.

## Precipitation seasonality effects on ice core isotope records

W. J. van de Berg et al.

Title Page

Abstract

Introduction

Conclusions

References

Tables

Figures

◀

▶

◀

▶

Back

Close

Full Screen / Esc

Printer-friendly Version

Interactive Discussion



The mean precipitation profile temperature ( $T_{pp}$ ) is the mean temperature ( $T_z$ ) convoluted with the vertical condensation profile,

$$T_{pp} = \frac{1}{P} \int_0^{\infty} T_z \int_0^T C_{tz} dt dz. \quad (2)$$

This temperature  $T_{pp}$  is a measure of the mean atmospheric temperature. Like the temperature at a fixed level, for example, 500 hPa, it gives the mean temperature for the period covered. In contrast to the temperature at a fixed level, which is valid only for that point,  $T_{pp}$  is the weighted average over the elevations at which precipitation has formed. So,  $T_{pp}$  includes the spatial differences in the vertical distribution of condensation. The difference between  $T_{2m}$  and  $T_{pp}$  reflects the difference between the temperature near the surface and the part of the atmosphere that is relevant for precipitation formation.

Differences between  $T_c$  and  $T_{pp}$  are due to the temporal variability of precipitation and condensation and originate from two sources. Firstly, the atmospheric temperature during precipitation events deviates from the mean temperature for that time of the year ( $dT_{event}$ ). Secondly, the precipitation events are unequally distributed over the year ( $dT_{seas}$ ). To calculate  $dT_{event}$ , the difference between  $T_{pp}$  and  $T_c$  is derived for each individual month, and this difference is weighted averaged over the whole period, thus

$$dT_{event} = \frac{1}{P} \sum (T_c - T_{pp})_{month} \cdot P_{month}. \quad (3)$$

The effect of precipitation seasonality causes the remaining difference between  $T_{pp}$  and  $T_c$ . A weighted average is used for  $dT_{event}$ , because  $T_c$  can be unrepresentative in months with very little precipitation. Using a normal average for  $dT_{event}$  would, therefore, lead to erroneous estimates of  $dT_{event}$  and subsequently  $dT_{seas}$ . However, using a weighted average causes  $dT_{event}$  to be affected by the precipitation seasonality, since  $dT_{event}$  is generally larger during winter than during summer. As will be shown later, this has little impact on the results.

## Precipitation seasonality effects on ice core isotope records

W. J. van de Berg et al.

Title Page

Abstract

Introduction

Conclusions

References

Tables

Figures

⏪

⏩

◀

▶

Back

Close

Full Screen / Esc

Printer-friendly Version

Interactive Discussion



Analogous to  $T_c$  (Eq. 1), a mean 2 m temperature can be derived for precipitation events ( $T_{2m,p}$ ) with

$$T_{2m,p} = \frac{1}{P} \int_0^T T_{2m,t} P_t dt, \quad (4)$$

in which  $T_{2m,t}$  is the 2 m temperature at time  $t$ . The difference between  $T_{2m,p}$  and the mean  $T_{2m}$  is solely due to temporal precipitation variability. The effects of seasonality and short term variability on  $T_{2m,p}$  can be isolated similarly as in Eq. (3).

### 2.3 Discussion of example profiles

Figure 1a shows three example profiles of mean temperature (solid) and mean condensation temperature (dashed). The two inland temperature profiles, starting at 2.8 km (South Dome) and 3 km (NorthGRIP) height, show the well known surface inversion layer, which is stronger at NorthGRIP than at South Dome. At these two locations, the mean condensation temperature is higher than the mean temperature for the whole column. Hence, precipitation occurs during warmer than average conditions, or during the warmer part of the year. At the sea point (65° N, 30° W), a stable boundary layer is not formed due to the presence of warm ocean water. Furthermore, in a 1 km deep layer centered at around 2 km elevation, a significant contribution of convective precipitation (Fig. 1b) lowers the condensation temperature below the mean temperature. Convection is forced by large vertical temperature gradients. With a sea surface temperature that is almost constant, convective precipitation then falls during periods in which the atmosphere is colder than average. Due to the generally warmer conditions over sea, evaporation of precipitation also is a more important process: the precipitation flux at 500 m is 10 % larger than the amount of precipitation that reaches the surface. Over the Greenland ice sheet, convective precipitation as well as evaporation of precipitation are both of limited importance: all precipitation is formed by large scale dynamic or topographic lifting.

## Precipitation seasonality effects on ice core isotope records

W. J. van de Berg et al.

Title Page

Abstract

Introduction

Conclusions

References

Tables

Figures

⏪

⏩

◀

▶

Back

Close

Full Screen / Esc

Printer-friendly Version

Interactive Discussion



## Precipitation seasonality effects on ice core isotope records

W. J. van de Berg et al.

Title Page

Abstract

Introduction

Conclusions

References

Tables

Figures

⏪

⏩

◀

▶

Back

Close

Full Screen / Esc

Printer-friendly Version

Interactive Discussion



Although the two inland examples appear rather similar, at NorthGRIP the precipitation is formed closer to the surface than at South Dome. The mean condensation elevation at South Dome and NorthGRIP is 4.54 and 4.29 km elevation, respectively. The atmosphere above NorthGRIP is colder than above South Dome, so this lower precipitation origin reduces the difference of  $T_c$  between both sites (249.7 and 252.6 K, respectively). The difference in  $T_{2m}$  between these two sites is 10.7 K.

### 3 Contemporary climate

#### 3.1 Mean condensation temperature

The spatial patterns of  $T_{2m}$ , 500 hPa temperature ( $T_{500hPa}$ ) and  $T_c$ , averaged for 1960–1989, are examined in Fig. 2. Figure 2a shows mean  $T_{2m}$  as simulated by RACMO2. It shows well known features, such as a north-south temperature gradient over the ocean, where the 271 K isotherm demarcates the winter extent of the sea ice. Over Greenland, isotherms follow the elevation contour lines combined with a north-south gradient. Longitudinal gradients are also visible, south-east Greenland being warmer than south-west Greenland, and north-west Greenland being warmer than north-east Greenland.

Compared to  $T_{2m}$ , mean  $T_c$  (Fig. 2b) is much less variable. Gradients over the ocean are largely reduced, becoming even smaller than the gradient in  $T_{500hPa}$ . The difference between  $T_c$  and  $T_{2m}$  exceeds 20 K over warm ocean water, but disappears over the ice covered Arctic ocean. The mean condensation altitude decreases towards higher latitudes, counterbalancing the effect of lower air temperatures. More pronounced gradients in  $T_c$  are found over Greenland, where topography is the primary factor determining the mean condensation temperature; latitude is of lesser importance.

#### 3.2 Factors determining the condensation temperature

Two factors determine the difference between  $T_{2m}$  and  $T_c$  (Fig. 2), namely, spatial and temporal temperature differences. Figure 3a shows the difference between the mean

temperature of the air in which the condensation occurs ( $T_{pp}$ ) and  $T_{2m}$ . As visible in Fig. 1b, condensation is unevenly distributed in the troposphere, which is included in the calculation of  $T_{pp}$  (see Eq. 2). Similarly, the effective condensation altitude is the weighted average of the condensation altitude.

Vertical temperature differences explain most of the difference between  $T_c$  and  $T_{2m}$  (Fig. 2), especially for warmer locations such as over the Atlantic Ocean. Over the ocean, the effective condensation altitude decreases with latitude, largely balancing the latitudinal temperature gradient. South of Iceland, the effective condensation altitude is about 2.9 km, near Spitsbergen it is about 1.9 km. Note that  $T_{pp}$  is not always lower than  $T_{2m}$ . The effective condensation elevation increases less with topography than the topography itself. As a result, it is situated relatively close to the surface over the higher parts of the ice sheet. In combination with the strong surface based temperature inversion, which is common for the northern GrIS, this causes  $T_{pp}$  to be equal to or even slightly higher than  $T_{2m}$ .

The remainder of the difference between  $T_c$  and  $T_{2m}$  is determined by temporal variability, and the maximum impact is about 5 K. The effect of temporal variability is either due to short-term variability ( $dT_{event}$ , Fig. 3b) or due to precipitation seasonality ( $dT_{seas}$ , Fig. 3c). A positive  $dT_{event}$  (Fig. 3b) implies that days with precipitation have higher atmospheric temperatures than average for that specific time of the year.  $T_{2m}$  is in general higher on days with precipitation, because precipitation coincides with cloudy conditions and usually also with enhanced winds, which both reduce the strength of the near-surface temperature inversion. This effect on the mean  $T_{2m}$  during precipitation can be up to 8 K (Fig. S2b). However, the spatial patterns in atmospheric  $dT_{event}$  are different to those for  $T_{2m}$   $dT_{event}$ . Moreover, little condensation occurs in the shallow atmospheric boundary layer;  $dT_{event}$  is mainly caused by other processes.  $dT_{event}$  becomes significant if precipitation events are associated with certain large-scale flow patterns. For most of Greenland, precipitation occurs when warm, moist air from the south flows over the ice sheet. The exception to this pattern is north Greenland, where  $dT_{event}$  is negative. This part of Greenland is on the lee side of the ice cap for warm air

## Precipitation seasonality effects on ice core isotope records

W. J. van de Berg et al.

[Title Page](#)[Abstract](#)[Introduction](#)[Conclusions](#)[References](#)[Tables](#)[Figures](#)[⏪](#)[⏩](#)[◀](#)[▶](#)[Back](#)[Close](#)[Full Screen / Esc](#)[Printer-friendly Version](#)[Interactive Discussion](#)

moving northward. Warm, northward moving air is thus descending here, and therefore too dry to generate precipitation. Precipitation has to come from the Arctic Ocean, which results in colder atmospheric conditions during precipitation events.

Over most of Greenland and the sea-ice covered ocean, seasonality has a warming impact on  $T_c$  (Fig. 3c). Summer precipitation exceeds winter precipitation, and the effect of seasonality is strongest for dry and cold locations. The effect of inter-annual variability on  $dT_{\text{seas}}$  is negligible. Besides the temperature-moisture effect – cold air carries less moisture, and produces less precipitation – sea ice is an important factor. Sea ice shields the atmosphere from an effective exchange of moisture and energy with the ocean. It also allows the build-up of a surface inversion, which stabilizes the atmosphere and prevents vertical mixing. As a result, the winter months are dryer than the summer period over the sea ice. Over the northern Atlantic Ocean, seasonality has a cooling effect on  $T_c$ . Here, most of the precipitation is due to cyclonic activity, which is significantly stronger during the winter period than in summer. Since south-east Greenland receives most of its precipitation by cyclones that develop at the southern tip of Greenland and travel to the north-east,  $dT_{\text{seas}}$  is negative in this coastal region, too.

## 4 Eemian changes

In the previous section, the processes that influence the condensation temperature in the present climate have been discussed. In this section it will be shown how these processes might have been different during the Eemian by comparing results of the ECHO-G model for Eemian and preindustrial conditions. For a description of the ECHO-G model setup and simulations, see Sect. 2.1. Simulations driven by the same GCM are required for a consistent analysis of Eemian changes, otherwise model dependent differences will interfere with the results presented. Therefore, the differences between the realization of preindustrial climate from RACMO2 driven by ECHO-G and the realization of recent-past (1960–1989) climate driven by ERA-40 are analyzed first. As shown in Fig. S1, the preindustrial simulation is a few degrees colder than the

### Precipitation seasonality effects on ice core isotope records

W. J. van de Berg et al.

Title Page

Abstract

Introduction

Conclusions

References

Tables

Figures



Back

Close

Full Screen / Esc

Printer-friendly Version

Interactive Discussion



## Precipitation seasonality effects on ice core isotope records

W. J. van de Berg et al.

Title Page

Abstract

Introduction

Conclusions

References

Tables

Figures

⏪

⏩

◀

▶

Back

Close

Full Screen / Esc

Printer-friendly Version

Interactive Discussion

recent-past simulation (Fig. S1a), leading to a lower  $T_{pp}$  (Fig. S1b) and  $T_c$  (Fig. S1c). The preindustrial climate was colder than the recent-past climate due to the absence of human induced climate warming, but this figure shows that ECHO-G has a cold bias over Greenland. In the preindustrial climate realization,  $T_{2m}$  decreased more than  $T_{pp}$  in Greenland (Fig. S1d). The contributions of  $dT_{event}$  and  $dT_{seas}$  to preindustrial  $T_c$ , however, remain similar to the recent-past contribution (Fig. S1e, f). A counterbalancing pattern is visible in North Greenland, where  $dT_{seas}$  decreases and  $dT_{event}$  increases, suggesting that North Greenland receives less precipitation from the Arctic Ocean in the preindustrial simulation. Despite the differences, the ECHO-G driven simulation provide a realistic realization of the preindustrial climate of Greenland.

Figure 4 shows the changes in  $T_{2m}$ ,  $T_{500hPa}$ ,  $T_c$  and the difference between  $T_{2m}$  and  $T_c$  during the Eemian compared to the preindustrial climate. A modest near surface warming of up to 1 K is simulated for Greenland (Fig. 4a). For large areas along the southern coastal margins, this warming is not significant. This significance ( $2\sigma$ ) is derived using the inter-annual variability in the temperature; other processes causing uncertainty, for example, decadal variability or uncertainties in the GCM climate, can not be easily quantified. The simulated annual mean warming is the result of strong summer warming, up to 3 K, and winter and spring cooling. A similar annual mean warming and increased amplitude of the seasonal temperature cycle is found for the free atmosphere. For example, the annual mean  $T_{500hPa}$  rises by 0.3 to 1.2 K over Greenland (Fig. 4a), while summer  $T_{500hPa}$  rises by 2 to 4 K. The enhanced seasonal temperature cycle is caused by the enhanced summer insolation. This additional insolation is efficiently absorbed by the earth and released to the atmosphere, since the Northern Hemisphere has a large fraction of land. Although the ocean surface has a lower albedo than land, land has a limited effective heat capacity, allowing the land surface temperature to respond fast to enhanced insolation. Eemian Northern Hemisphere winter and spring temperatures are below preindustrial values; during the Eemian Northern Hemisphere winter, the earth passes through the aphelion. In the current orbit, the Earth passes through perihelion during the Northern Hemisphere winter. The RACMO2 and

## Precipitation seasonality effects on ice core isotope records

W. J. van de Berg et al.

Title Page

Abstract

Introduction

Conclusions

References

Tables

Figures

⏪

⏩

◀

▶

Back

Close

Full Screen / Esc

Printer-friendly Version

Interactive Discussion

ECHO-G results indicate that during the Eemian the altered orbital parameters caused a larger seasonality, but did not cause a significantly warmer climate. Moreover, little correspondence exists between the  $T_{2m}$  temperature change and that in the free atmosphere, a result of different mechanisms driving free atmosphere and near-surface warming. Especially over the ocean the differences are outspoken.  $T_{2m}$  over the ocean is controlled by the water temperature, and its changes reflect changes in ocean circulation and ice cover. A warming of Fram Strait area is simulated, due to reduced sea ice cover, and a cooling in the Labrador Sea, due to a reduced entrainment of warm Atlantic water.

The change in condensation temperature  $T_c$  in Fig. 4b is on average larger than that in  $T_{2m}$  and  $T_{500hPa}$  and ranges from  $-1$  to  $+3$  K. Whereas insignificant changes are found over the Atlantic Ocean, higher  $T_c$  is found over most of Greenland and its surrounding seas with seasonal sea ice cover, with a maximum increase over North Greenland. Again, little spatial correspondence exists between changes in  $T_c$  and either  $T_{2m}$  and  $T_{500hPa}$ , indicating the different mechanisms that caused these changes. For large parts of the GrIS, the change in  $T_c$  is not significantly different from the change in  $T_{2m}$  (Fig. 4c). Only for north and central Greenland,  $T_c$  increased more than  $T_{2m}$ , including the areas around the GRIP, NorthGRIP and NEEM ice cores. In contrast, the  $T_c$  increase is significantly smaller than the  $T_{2m}$  increase for part of the eastern coast of Greenland, including the Renland ice cap. The change difference between  $T_c$  and  $T_{500hPa}$  over Greenland is comparable to Fig. 4c (Fig. S3b). For the North facing northern part of GrIS, a significantly larger increase of  $T_c$  than  $T_{500hPa}$  is found and a significantly smaller and even negative change is found along the southeastern coast.

### Factors determining Eemian changes

In Sect. 3.2, the difference between  $T_c$  and  $T_{2m}$  was attributed to differences in  $T_{2m}$  and  $T_{pp}$ ,  $dT_{event}$  and  $dT_{seas}$ . Figure 5 shows how these contributions differ between the Eemian and Preindustrial climate. Changes in the difference between  $T_{pp}$  and  $T_{2m}$  (Fig. 5a) are significant, especially over the ocean, indicating that the ocean surface

## Precipitation seasonality effects on ice core isotope records

W. J. van de Berg et al.

Title Page

Abstract

Introduction

Conclusions

References

Tables

Figures

⏪

⏩

◀

▶

Back

Close

Full Screen / Esc

Printer-friendly Version

Interactive Discussion

cooling did not occur with a similar cooling of  $T_{pp}$ . Over Greenland, the change is slightly negative, with the largest changes in areas with enhanced refreezing. Snow melt and subsequent refreezing is an effective way to bring energy into the snow pack. This energy is released to the atmosphere during the winter season, causing a small but clear surface warming signal. Over land, the changes in the difference between  $T_{500hPa}$  and  $T_{pp}$  (Fig. S3c) are comparable to those between  $T_{2m}$  and  $T_{pp}$ , shown in Fig. 5a. Over sea,  $T_{pp}$  became lower than  $T_{500hPa}$  by up to 3K; the spatial patterns relate closely to the spatial patterns of Eemian ocean surface cooling (Fig. 4a). The changes in the temperature difference between “wet” and average conditions ( $dT_{event}$ , Fig. 5b) are relatively minor.

The main reason for Eemian  $T_c$  to rise more than  $T_{2m}$  is precipitation seasonality ( $dT_{seas}$ , Fig. 5c). For most of Greenland, in the present climate precipitation events are biased to the warmer part of the year (Fig. 3c), and this bias is enhanced in the Eemian. The spatial patterns in Figs. 3c and 5c are therefore comparable. Remarkably, the cooling of the Labrador Sea coincides with a strong increase of the regional precipitation seasonality.

The changes in precipitation seasonality has two components: a temperature and a precipitation contribution. Enhanced Eemian temperature seasonality can alter  $T_c$  in places where the precipitation is already unevenly distributed over the year. This enhances  $T_c$  by up to 1 K in northern Greenland, Ellesmere Island and the Labrador Sea and decreases it along the southeastern coast of Greenland (not shown). This pattern does not look similar to the present-day seasonality effect (Fig. 3c). This is because most Eemian warming occurs during late summer and early fall (July to October), lagging the insolation anomaly, which peaks in June. Winter and early spring (December to May) were on average colder in the Eemian. Hence, a positive effect of precipitation seasonality on  $T_c$  for preindustrial conditions does not necessarily cause a similar effect for the Eemian. The second component, changes in the precipitation seasonality, is the main contribution to changes in  $dT_{seas}$ . The effect of the enhanced precipitation seasonality on  $T_c$  is shown in Fig. 5d and causes an increase of  $T_c$  of up to 1.5 K in

northern Greenland. The spatial pattern is very similar to the contribution of  $dT_{\text{seas}}$  to  $T_c$  for the preindustrial climate (Fig. 5c).

The role of precipitation seasonality is further visualized in Fig. 6. For two deep ice core drilling sites, NorthGRIP and NEEM, the mean monthly values of precipitation,  $T_{2m}$  and  $T_c$  are shown for the preindustrial and Eemian simulations. For both sites, a significant Eemian summer warming is simulated, which is most pronounced in  $T_{2m}$ . A significant cooling of  $T_c$  is visible for the Eemian winter, while  $T_{2m}$  remains almost unchanged. If precipitation variability is neglected,  $T_{2m}$  rises more than  $T_c$  for the Eemian. However, Eemian late summer precipitation is significantly enhanced at the expense of winter precipitation. This causes  $T_c$  to rise more than  $T_{2m}$ .

Although the pattern with strong Eemian warming of  $T_c$  over North Greenland (Fig. 4b) might suggest that Arctic summer sea ice is of importance, it is unlikely that this is the case. Firstly, the relative increase of summer precipitation is for a significant part due to reduced winter precipitation. Reduced winter precipitation is due to colder winter conditions on which sea ice has little impact. Secondly, increased summer precipitation is a logical result of warmer conditions and the spatial pattern does not show that most increase occurs in the vicinity of the Arctic Ocean. West Greenland, far away from the Arctic Ocean, has a comparable increase of  $T_c$  due to enhanced precipitation seasonality as North Greenland (Fig. 5d). However, the areas with significant precipitation enhancement of  $T_c$  (Fig. 4c) are without exception areas with already significant precipitation seasonality in the preindustrial climate. In these areas, more than 45 % of the precipitation falls between June and September, a number which further increased in the Eemian climate. Due to this strong “background” precipitation seasonality, the enhanced temperature seasonality acts positively on  $T_c$ ; in other areas the enhanced temperature seasonality has no effect on  $T_c$ . Concluding, changes in  $T_c$  thus depend on the precipitation seasonality and changes therein and on changes in the temperature seasonality; all these three components are equally important.

## Precipitation seasonality effects on ice core isotope records

W. J. van de Berg et al.

Title Page

Abstract

Introduction

Conclusions

References

Tables

Figures



Back

Close

Full Screen / Esc

Printer-friendly Version

Interactive Discussion



## 5 Conclusions

Using output of the regional atmospheric climate model RACMO2, the impact of local and regional climate conditions on  $T_c$  is investigated for current, preindustrial and Eemian (125 kyr BP) climate. In all cases, precipitation seasonality is an important factor for the local  $T_c$ . For most of Greenland, precipitation is biased high in the summer months, and isotopic records are mostly influenced by summer precipitation.

Our model results show that the condensation temperature ( $T_c$ ) does not clearly relate to near-surface, e.g.  $T_{2m}$  or free atmosphere, e.g.  $T_{500hPa}$ , temperatures. This is firstly due to the mean elevation at which precipitation is formed. Most precipitation originates from the lower troposphere, but is not influenced by the boundary layer processes that govern  $T_{2m}$ .  $T_c$  does not relate to  $T_{500hPa}$  because of the spatial variation of the typical condensation elevation as a result of atmospheric temperature and surface topography. Moreover, precipitation seasonality causes  $T_c$  to reflect mostly summer conditions;  $T_c$  is thus higher than the average temperature of the atmospheric levels from which this precipitation originates.

Compared to the preindustrial climate the ECHO-G/RACMO2 realization of the Eemian climate has only limited annual warming (up to 1 K) over GrIS and the Northern Hemisphere. Nevertheless, the model output compares well with paleoclimate records outside Greenland. Despite the limited surface warming,  $T_c$  over Northern Greenland was much higher during the Eemian than in preindustrial conditions. Enhanced precipitation seasonality compared to the preindustrial and current climate causes  $T_c$  to rise more than near-surface and free atmosphere temperature. As a result, the increase of  $T_c$  (–1 to 3 K) exceeds that of  $T_{2m}$  or  $T_{500hPa}$  (both 0 to 1 K). These results compare well with the estimated precipitation effect on Eemian  $\delta^{18}O$  as presented by Masson-Delmotte et al. (2011). The results shown here are based on climate realizations of one GCM/RCM combination, so besides the study by Masson-Delmotte et al. (2011) there is no additional evidence that the results presented here are deterministic. However, the GCM/RCM combination of ECHO-G and RACMO2 provides a realistic climate

CPD

9, 269–296, 2013

### Precipitation seasonality effects on ice core isotope records

W. J. van de Berg et al.

Title Page

Abstract

Introduction

Conclusions

References

Tables

Figures

⏪

⏩

◀

▶

Back

Close

Full Screen / Esc

Printer-friendly Version

Interactive Discussion



realizations; this study, therefore, shows that the impact of changing precipitation seasonality on  $T_c$  can not be excluded a priori.

In conclusion, the condensation temperature is an important factor for isotope physics, but many more processes play a role, for example, the temperature of the moisture source. It is, therefore, not straightforward to relate the observed sensitivity of  $T_c$  to precipitation seasonality to a sensitivity of isotopic properties, like  $\delta^{18}\text{O}$ , to precipitation seasonality. This study, however, shows that Eemian isotopic proxies from ice cores are affected by changes in precipitation seasonality. The induced uncertainty due to possible changes in precipitation seasonality in Eemian temperature estimates based on ice core data is up to 2 K.

**Supplementary material related to this article is available online at:**

**<http://www.clim-past-discuss.net/9/269/2013/cpd-9-269-2013-supplement.pdf>**

*Acknowledgements.* George Hoffman is thanked for valuable discussions. This work was sponsored by the Stichting Nationale Computerfaciliteiten (National Computing Facilities Foundation, NCF) for the use of supercomputer facilities, with financial support from the Nederlandse Organisatie voor Wetenschappelijk Onderzoek (Netherlands Organization for Scientific Research, NWO).

## References

- Dansgaard, W.: Stable isotopes in precipitation, *Tellus*, 16, 436–468, 1964. 270
- EPICA community members: Eight glacial cycles from an Antarctic ice core, *Nature*, 429, 623–628, 2004. 271
- Ettema, J., van den Broeke, M. R., van Meijgaard, E., van de Berg, W. J., Bamber, J. L., Box, J. E., and Bales, R. C.: Higher surface mass balance of the Greenland ice sheet revealed by high-resolution climate modeling, *Geophys. Res. Lett.*, 36, doi:10.1029/2009GL038110, 2009. 273
- Ettema, J., van den Broeke, M. R., van Meijgaard, E., and van de Berg, W. J.: Climate of the Greenland ice sheet using a high-resolution climate model – Part 2: Near-surface climate and energy balance, *The Cryosphere*, 4, 529–544, doi:10.5194/tc-4-529-2010, 2010a. 273

## Precipitation seasonality effects on ice core isotope records

W. J. van de Berg et al.

Title Page

Abstract

Introduction

Conclusions

References

Tables

Figures



Back

Close

Full Screen / Esc

Printer-friendly Version

Interactive Discussion



---

**Precipitation  
seasonality effects  
on ice core isotope  
records**

---

W. J. van de Berg et al.

---

[Title Page](#)[Abstract](#)[Introduction](#)[Conclusions](#)[References](#)[Tables](#)[Figures](#)[⏪](#)[⏩](#)[◀](#)[▶](#)[Back](#)[Close](#)[Full Screen / Esc](#)[Printer-friendly Version](#)[Interactive Discussion](#)

- Ettema, J., van den Broeke, M. R., van Meijgaard, E., van de Berg, W. J., Box, J. E., and Steffen, K.: Climate of the Greenland ice sheet using a high-resolution climate model – Part 1: Evaluation, *The Cryosphere*, 4, 511–527, doi:10.5194/tc-4-511-2010, 2010b. 272, 273
- Francis, D. R., Wolfe, A. P., Walker, I. R., and Miller, G. H.: Interglacial and Holocene temperature reconstructions based on midge remains in sediments of two lakes from Baffin Island, Nunavut, Arctic Canada, *Palaeogeogr. Palaeoclimatol.*, 236, 107–124, 2006. 274
- Helsen, M. M., van de Wal, R. S. W., van den Broeke, M. R., Kerstel, E. R. T., Masson-Delmotte, V., Meijer, H. A. J., Reijmer, C. H., and Scheele, M. P.: Modelling the isotopic composition of snow using backward trajectories: a particular precipitation event in Dronning Maud Land, Antarctica, *Ann. Glaciol.*, 39, 293–299, 2004. 271
- Helsen, M. M., van de Wal, R. S. W., van den Broeke, M. R., Masson-Delmotte, V., Meijer, H. A. J., Scheele, M. P., and Werner, M.: Modeling the isotopic composition of Antarctic snow using backward trajectories: Simulation of snow pit records, *J. Geophys. Res.*, 111, D15109, doi:10.1029/2005JD006524, 2006. 271
- Johnsen, S. J., Clausen, H. B., Dansgaard, W., Fuhrer, K., Gundestrup, N., Hammer, C. U., Iversen, P., Jouzel, J., Stauffer, B., and Steffensen, J. P.: Irregular glacial interstadials recorded in a new Greenland ice core, *Nature*, 359, 311–314, 1992. 270
- Johnsen, S. J., Clausen, H. B., Dansgaard, W., Gundestrup, N. S., Hammer, C. U., Andersen, U., Anderson, K. K., Hvidberg, C. S., Dahl-Jensen, D., Steffensen, J. P., Shoji, H., Sveinbjörnsdóttir, A. E., White, J., Jouzel, J., and Fisher, D.: The  $\delta^{18}\text{O}$  record along the Greenland Ice Core Project deep ice core and the problem of possible Eemian climatic instability, *J. Geophys. Res.*, 102, 26397–26410, 1997. 271
- Jouzel, J., Alley, R. B., Cuffey, K. M., Dansgaard, W., Grootes, P., Hoffmann, G., Johnsen, S. J., Koster, R. D., Peel, D., Shuman, C. A., Stievenard, M., Stuiver, M., and White, J.: Validity of the temperature reconstruction from water isotopes in ice cores, *J. Geophys. Res.*, 102, 26471–26487, 1997. 271
- Kaspar, F. and Cubasch, U.: The climate of past interglacials, in: *Simulations of the Eemian Interglacial and the Subsequent Glacial Inception with a Coupled Ocean – Atmosphere General Circulation Model*, Elsevier, 2007. 271, 273
- Kaspar, F., Köhl, N., Cubasch, U., and Litt, T.: A model-data comparison of European temperatures in the Eemian interglacial, *Geophys. Res. Lett.*, 32, L11703, doi:10.1029/2005GL022456, 2005. 271, 273, 274

## Precipitation seasonality effects on ice core isotope records

W. J. van de Berg et al.

Title Page

Abstract

Introduction

Conclusions

References

Tables

Figures

⏪

⏩

◀

▶

Back

Close

Full Screen / Esc

Printer-friendly Version

Interactive Discussion



- Kaspar, F., Spangehl, T., and Cubasch, U.: Northern hemisphere winter storm tracks of the Eemian interglacial and the last glacial inception, *Clim. Past*, 3, 181–192, doi:10.5194/cp-3-181-2007, 2007. 273
- Legutke, S. and Maier-Reimer, E.: Climatology of the ECHO-G Global Ocean–Sea Ice General Circulation Model, Technical Report 21, Deutsches Klimarechenzentrum, Hamburg, 1999. 273
- Legutke, S. and Voss, R.: The Hamburg atmosphere-ocean coupled circulation model ECHO-G, Technical Report 18, Deutsches Klimarechenzentrum, Hamburg, 1999. 273
- Masson-Delmotte, V., Braconnot, P., Hoffmann, G., Jouzel, J., Kageyama, M., Landais, A., Lejeune, Q., Risi, C., Sime, L., Sjolte, J., Swingedouw, D., and Vinther, B.: Sensitivity of interglacial Greenland temperature and  $\delta^{18}\text{O}$ : ice core data, orbital and increased  $\text{CO}_2$  climate simulations, *Clim. Past*, 7, 1041–1059, doi:10.5194/cp-7-1041-2011, 2011. 271, 285
- NorthGRIP community members: High resolution climate record of the Northern Hemisphere reaching into last interglacial period, *Nature*, 431, 147–151, 2004. 270, 271
- Otto-Bliesner, B. L., Marshall, S. J., Overpeck, J. T., Miller, G. H., Hu, A., and members, C. L. I. P.: Simulating Arctic climate warmth and icefield retreat in the last interglaciation, *Science*, 311, 1751–1753, 2006. 271
- Petit, J. R., Jouzel, J., Raynaud, D., Barnola, N. I., Basile, I., Bender, M., Chappallaz, J., Davis, M., Delaygue, G., Delmotte, M., Kotlyakov, V. M., Legrand, M., Lipenkov, V. Y., Lorius, C., Pépin, L., Ritz, C., Saltzman, E., and Stievenard, M.: Climate and atmospheric history of the past 420 000 years from the Vostok ice core, Antarctica, *Nature*, 399, 429–436, 1999. 271
- Reeh, N.: Parameterization of melt rate and surface temperature on the Greenland ice sheet, *Polarforschung*, 59, 113–128, 1991. 273
- Reijmer, C., van Meijgaard, E., and van den Broeke, M.: Numerical Studies with a regional atmospheric climate model based on changes in the roughness length for momentum and heat over Antarctica, *Bound.-Lay. Meteorol.*, 111, 313–337, 2004. 272
- Shuman, C. A., Bromwich, D. H., Kipfstuhl, J., and Schwager, M.: Multiyear accumulation and temperature history near the North Greenland Ice Core Project site, north central Greenland, *J. Geophys. Res.*, 106, 33853–33866, 2001. 271
- Sjolte, J., Hoffmann, G., Johnsen, S. J., Vinther, B. M., and Masson-Delmotte, V.: Modeling the water isotopes in Greenland precipitation 1959–2001 with the meso-scale model REMO-iso, *J. Geophys. Res.*, 116, D18105, doi:10.1029/2010JD015287, 2011. 271

---

## Precipitation seasonality effects on ice core isotope records

W. J. van de Berg et al.

---

[Title Page](#)[Abstract](#)[Introduction](#)[Conclusions](#)[References](#)[Tables](#)[Figures](#)[⏪](#)[⏩](#)[◀](#)[▶](#)[Back](#)[Close](#)[Full Screen / Esc](#)[Printer-friendly Version](#)[Interactive Discussion](#)

- Steen-Larsen, H. C., Masson-Delmotte, V., Sjolte, J., Johnsen, S. J., Vinther, B. M., Bréon, F.-M., Clausen, H. B., Dahl-Jensen, D., Falourd, S., Fettweis, X., Gallée, H., Jouzel, J., Kageyama, M., Lerche, H., Minster, B., Picard, G., Punge, H. J., Risi, C., Salas, D., Schwander, J., Steffen, K., Sveinbjörnsdóttir, A. E., Svensson, A., and White, J.: Understanding the climate signal in the water stable isotope records from the NEEM shallow firn/ice cores in northwest Greenland, *J. Geophys. Res.*, 116, D06108, doi:10.1029/2010JD014311, 2011. 271
- Undén, P., Rontu, L., Järvinen, H., Lynch, P., Calvo, J., Cats, G., Cuxart, J., Eerola, K., Fortelius, C., Garcia-Moya, J. A., Jones, C., Lenderink, G., McDonald, A., McGrath, R., Navascues, B., Woetman Nielsen, N., Ødegaard, V., Rodriguez, E., Rummukainen, M., Rõõm, R., Sattler, K., Hansen Sass, B., Savijärvi, H., Wichers Schreur, B., Sigg, R., The, H., and Tijm, A. B. C.: The High Resolution Limited Area Model, Hirlam-5 scientific documentation, Swedish Meteorological and Hydrological Institute, Norrköping, Sweden, 2002. 272
- Uppala, S. M., Kållberg, P. W., Simmons, A. J., Andrae, U., Bechtold, V. D. C., Fiorino, M., Gibson, J. K., Haseler, J., Hernandez, A., Kelly, G. A., Li, X., Onogi, K., Saarinen, S., Sokka, N., Allan, R. P., Andersson, E., Apre, K., Balmaseda, M. A., Beljaars, A. C. M., van de Berg, L., Bidlot, J., Bormann, N., Caires, S., Chevallier, F., and Dethof, A.: The ERA-40 reanalysis, *Q. J. Roy. Meteorol. Soc.*, 131, 2961–3012, 2005. 273
- van de Berg, W. J., van den Broeke, M. R., Ettema, J., van Meijgaard, E., and Kaspar, F.: Significant contribution of insolation to Eemian melting of the Greenland ice sheet, *Nat. Geosci.*, 4, 679–683, 2011. 271, 273
- van den Broeke, M. R., Bamber, J., Ettema, J., Rignot, E., Schrama, E., van de Berg, W. J., van Meijgaard, E., Velicogna, I., and Wouters, B.: Partitioning recent Greenland mass loss, *Science*, 326, 984–986, 2009. 273
- van Meijgaard, E., van Uft, L. H., van de Berg, W. J., Bosveld, F. C., van den Hurk, B. J. J. M., Lenderink, G., and Siebersma, A. P.: The KNMI regional atmospheric climate model RACMO version 2.1, Tech. Rep. 302, KNMI, De Bilt, The Netherlands, 2008. 272
- Werner, M., Mikolajewicz, U., Heimann, M., and Hoffmann, G.: Borehole versus isotope temperatures on Greenland: seasonality does matter, *Geophys. Res. Lett.*, 27, 723–726, 2000. 271
- White, P. W.: Physical Processes (CY23R4), Part IV, European Centre For Medium-Range Weather Forecasts (ECMWF), 2001. 272

## Precipitation seasonality effects on ice core isotope records

W. J. van de Berg et al.

**Table 1.** Climate parameters used in the various runs. The angle of the perihelion is calculated from the vernal equinox. For the simulation of present-day climate, a different routine was used to determine the position of the sun.

	Orbital parameters			Greenhouse gas concentrations		
	Eccentricity	Obliquity (°)	Angle of perihelion (°)	CO <sub>2</sub> (ppmv)	CH <sub>4</sub> (ppmv)	N <sub>2</sub> O (ppbv)
125 kyr BP	0.0400	23.79	127.3	270	630	160
Preindustrial	0.0167	23.44	282.7	270	600	270
Present-day		As observed		Varying as observed		

Title Page

Abstract

Introduction

Conclusions

References

Tables

Figures

◀

▶

◀

▶

Back

Close

Full Screen / Esc

Printer-friendly Version

Interactive Discussion



## Precipitation seasonality effects on ice core isotope records

W. J. van de Berg et al.

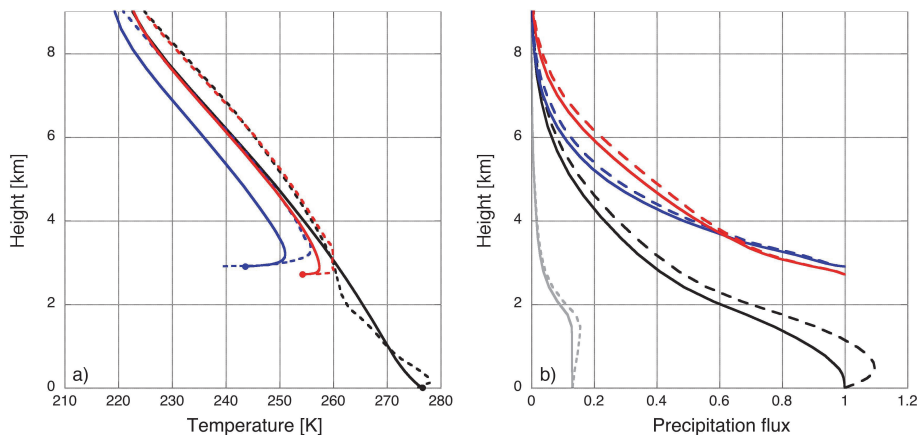


**Fig. 1.** (a) Average temperature profile (solid), 2 m temperature (line end dots) and mean temperature profile for precipitation events (dashed). (b) Vertical profile of precipitation flux. Net and total precipitation fluxes are drawn with a solid and dashed line, respectively. The profiles of northGRIP (75.1° N, 43.32° W), South Dome (62.5° N, 45° W) and a point over sea (65° N, 30° W) are shown in blue, red and black, respectively. The grey lines are the net and total convective precipitation for the point over sea. All values are scaled with the net precipitation.

Title Page

Abstract

Introduction

Conclusions

References

Tables

Figures

◀

▶

◀

▶

Back

Close

Full Screen / Esc

Printer-friendly Version

Interactive Discussion

## Precipitation seasonality effects on ice core isotope records

W. J. van de Berg et al.

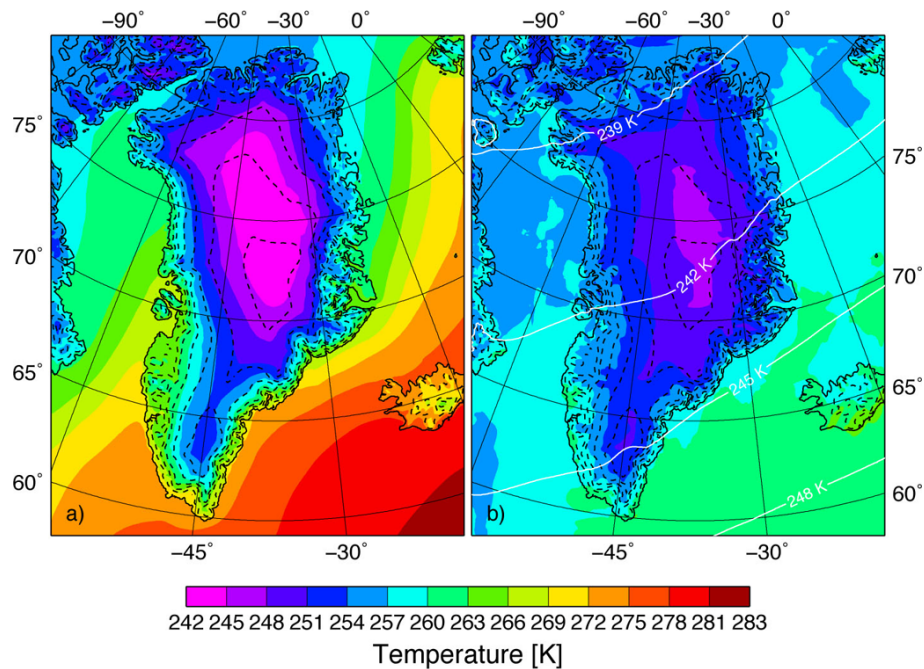


**Fig. 2.** Mean modeled 1960–1989 averages of (a)  $T_{2m}$ , (b)  $T_c$  and  $T_{500hPa}$  (white lines).

Title Page

Abstract

Introduction

Conclusions

References

Tables

Figures

◀

▶

◀

▶

Back

Close

Full Screen / Esc

Printer-friendly Version

Interactive Discussion

## Precipitation seasonality effects on ice core isotope records

W. J. van de Berg et al.

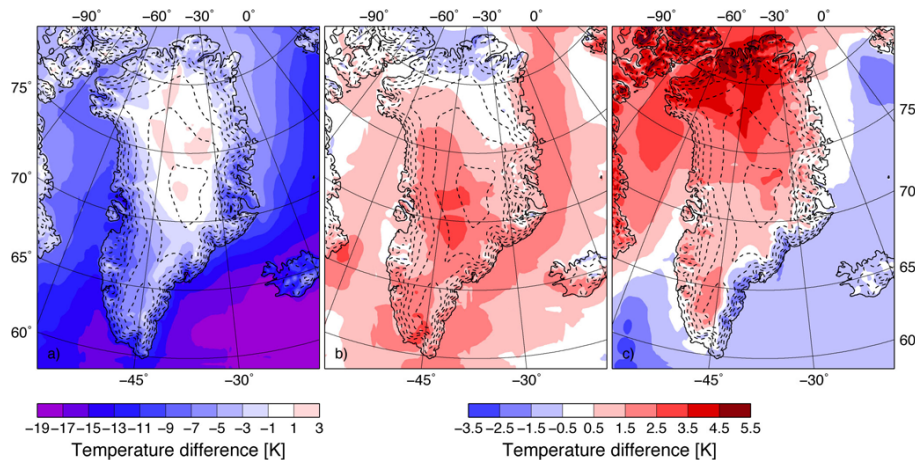


**Fig. 3.** Differences between  $T_c$  and  $T_{2m}$  for the current climate due to (a) differences between  $T_{pp}$  and  $T_{2m}$ ; (b) temperature differences between “wet” and mean conditions ( $dT_{event}$ ); (c) precipitation seasonality and interannual variability ( $dT_{seas}$ ).

Title Page

Abstract

Introduction

Conclusions

References

Tables

Figures

⏪

⏩

◀

▶

Back

Close

Full Screen / Esc

Printer-friendly Version

Interactive Discussion

## Precipitation seasonality effects on ice core isotope records

W. J. van de Berg et al.

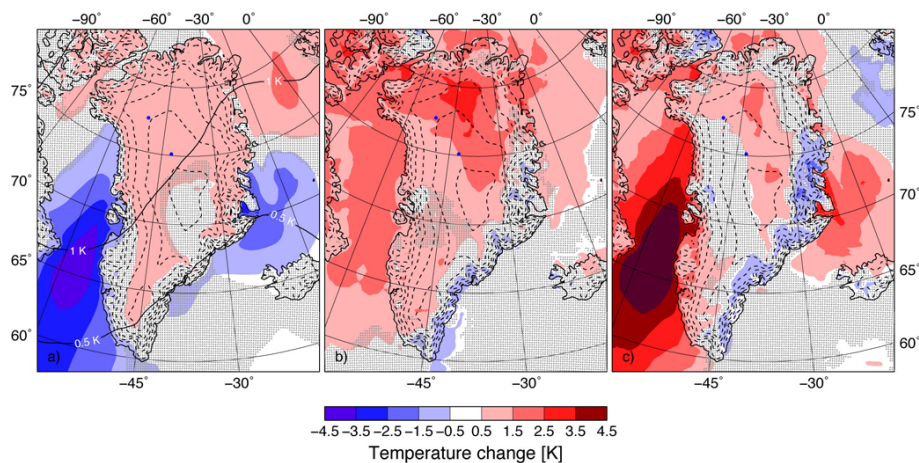


**Fig. 4.** Changes in the Eemian with respect to the preindustrial simulation for **(a)**  $T_{2m}$ ,  $T_{500hPa}$  (contours), **(b)**  $T_c$  and **(c)** the difference between  $T_c$  and  $T_{2m}$ . Areas with differences that fail to reach significance at  $2\sigma$  level are dotted (blue dots represent the locations of NorthGRIP and NEEM).

Title Page

Abstract

Introduction

Conclusions

References

Tables

Figures

◀

▶

◀

▶

Back

Close

Full Screen / Esc

Printer-friendly Version

Interactive Discussion

## Precipitation seasonality effects on ice core isotope records

W. J. van de Berg et al.

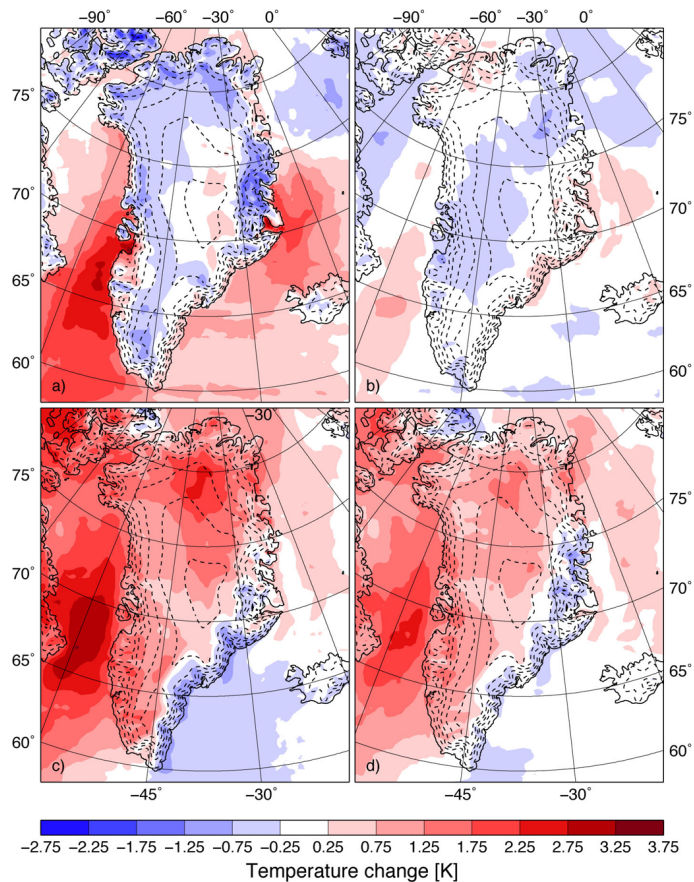


**Fig. 5.** Components of the changes in  $T_{2m}$  and  $T_c$ . **(a)** Change in difference between  $T_{pp}$  and  $T_{2m}$ . **(b)** Change in  $dT_{event}$ . **(c)** Change in  $dT_{seas}$ . **(d)** Change in  $T_c$  due to enhanced precipitation seasonality only.

Title Page

Abstract

Introduction

Conclusions

References

Tables

Figures

◀

▶

◀

▶

Back

Close

Full Screen / Esc

Printer-friendly Version

Interactive Discussion

## Precipitation seasonality effects on ice core isotope records

W. J. van de Berg et al.

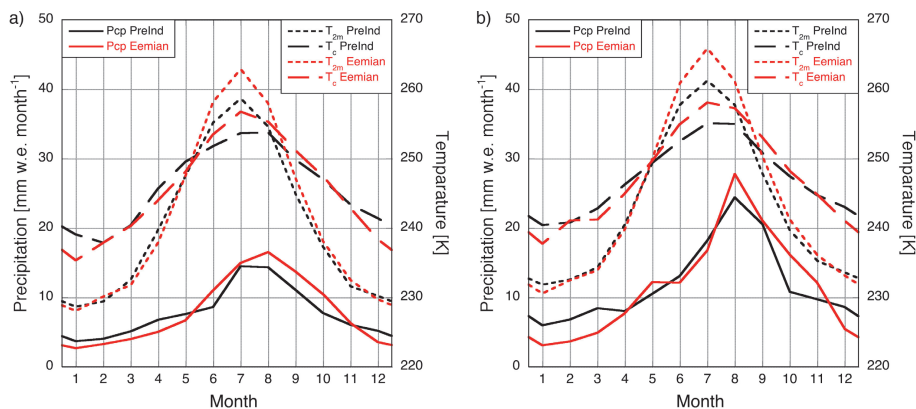


**Fig. 6.** Annual cycle of precipitation,  $T_{2m}$  and  $T_c$  for Preindustrial and Eemian conditions at **(a)** NorthGRIP (75.1° N, 42.32° W) and **(b)** NEEM (77.45° N, 51.06° W).

Title Page

Abstract

Introduction

Conclusions

References

Tables

Figures

◀

▶

◀

▶

Back

Close

Full Screen / Esc

Printer-friendly Version

Interactive Discussion